Fabrication of optical gratings through surface patterning of zirconium-based metallic glass by laser irradiation

著者	Rui Yamada, Naoyuki Nomura, Junji Saida, Akira Kawasaki
journal or publication title	Intermetallics
volume	93
page range	377-382
year	2017-11-11
URL	http://hdl.handle.net/10097/00126478

doi: 10.1016/j.intermet.2017.11.003

Fabrication of Optical Gratings through Surface Patterning of Zirconium-based Metallic Glass by Laser Irradiation

Rui Yamada[a], Naoyuki Nomura[b], Junji Saida[a], Akira Kawasaki[b]

[a]*Frontier Research Institute for Interdisciplinary Sciences (FRIS), Tohoku University, Sendai 980-8578, Japan*

[b]*Departments of Materials Science and Engineering, Tohoku University, Sendai 980-8578, Japan*

Abstract

Periodic lines with intervals ranging from ~220 μm down to ~27 μm were fabricated on the surface of $Zr_{55}Cu_{30}Al_{10}Ni_5$ metallic glass ribbon and disk samples by laser irradiation. The X-ray diffraction results indicated that both oxides (monoclinic ZrO_2, tetragonal ZrO_2) and crystallites ($Cu_{10}Zr_7$, $NiZr_2$) existed together with the amorphous phase on the surface of the laser-patterned metallic glass samples. The energy-dispersive X-ray spectroscopy of a cross section of a disk sample clearly showed that high amounts of aluminum (292% of the nominal composition) and oxygen were present in the laser-irradiated area, suggesting that Al_2O_3 formed on the surface of the laser-irradiated region. Reflective diffraction spots were observed from the fine grids with a grating period of ~27 μm, indicating the excellent periodicity and accuracy of the pattern in two dimensions on the surface of the metallic glass substrates. Calculation of the grating period using Bragg's law confirmed that the spots originated from the periodic patterns of the laser-irradiated lines. Along the lines, pairs of ridges and hollows with a height/depth of ~0.5 μm were observed; such specific morphology generated the diffraction spots as a reflective grating. We observed structural color gradation from the periodic fine grids under a fluorescent light. The present study showed that it is possible to prepare optical gratings on the surface of metallic glasses by laser irradiation more cheaply and easily than by conventional imprinting.

Keywords: metallic glass, laser irradiation, surface patterning, optical gratings, structural color

*Corresponding author. Tel.: +81-22-795-4488.

E-mail address: rui-yamada@fris.tohoku.ac.jp. (R. Yamada)

1. Introduction

Metallic glasses are attractive materials for several practical applications because of their excellent properties such as low elastic modulus with large elastic limit, super high strength, and high wear and corrosion resistance [1-4]. The most remarkable characteristic that metallic glasses exhibit is excellent formability in the supercooled liquid region. To date, many studies on the fabrication of microparts or larger products composed of metallic glasses by superplastic forming have been reported [5-7]. Meanwhile, the surface patterning of metallic glasses has been investigated with the aim of adding new functions (e.g., wetting, friction, absorption, and recording). For example, Li et al. [8] prepared micro-honeycomb structures with various pitches on the surface of $Zr_{35}Ti_{30}Cu_{8.25}Be_{26.75}$ metallic glass to tune its apparent friction coefficient. Fukuda and colleagues fabricated a nanodot array on the surface of $Pd_{39}Cu_{29}Ni_{13}P_9$ metallic glass to produce a bit-patterned medium [9].

One of the most interesting applications of metallic glasses with surface patterning is as optical gratings [10,11]. Metallic glasses inherently possess a smooth and shiny surface finish compared with that of their crystalline counterparts [12], which is expected to provide high-performance grating products than normal metal (e.g. pure Ni etc.) one. The high mechanical strength of metallic glasses would also broaden their application fields wider compared with conventional materials such as polydimethylsiloxane (PDMS) and polymethyl methacrylate (PMMA). Optical gratings require precise geometry on the scale of about several tens of micrometers down to nanometer size. Supercooled liquids are known to display excellent forming ability at such a microscopic scale range [13]. Chu et al. [10] fabricated gratings with periods of 600 and 1500 nm on $Pd_{40}Ni_{40}P_{20}$ metallic glass. Meanwhile, Saotome and co-

workers fabricated a diffraction grating with a 1-μm interval on the surface of $Pt_{48.75}Pd_{9.75}Cu_{19.5}P_{22}$ metallic glass [11]. In most cases, the precise patterning was attained by imprinting, which enables near-net-shape fabrication and is the most common method to prepare products with complicated shapes like optical gratings. However, imprinting has many drawbacks. Generally, imprinting requires precise molds, which are often difficult to fabricate. In addition, high surface finish at the micro/nanoscale is expensive. A currently used mold fabrication method is lithography, which allows high-accuracy preparation of detail shapes with high reproducibility [14]. However, the lithography process takes a long time because it involves many steps, like coating resist, exposure, development, etching, and stripping resist, and is also expensive. Another problem with imprinting is that it is difficult to release the final product from the mold. The mechanical/chemical damage of the product caused during release from the mold is also a big concern.

Meanwhile, the new demolding technique has currently proposed by Hasan *et al.* [15]. They demonstrated the nondestructive demolding and reusability of molds, utilizing the advantage of strain rate dependent strengthening of metallic glass supercooled liquids. Although the idea was unique, there are still some concerns to be worth noting. Even though the demolding was conducted in the supercooled liquid region, such a fast demolding rate (*i.e.* ~12 mm/s) may cause not only increasing the demolding stress but also, in the worst case, may lead to the fracture of the sample associated with shear-localization. The technical difficulty in demolding the sample from the mold in the supercooled liquid region is also a problem. From these backgrounds, imprinting is yet not an ideal way to prepare patterns on the surface of metallic glasses from an industrial point of view.

Recently, the use of laser technology in metallic glass research has been intensively studied [16]. Laser irradiation is purported to be an easy, fast, and cheap way to design the characteristics of metallic glasses. Much research in this vein, including surface modification [17], mechanical machining [18], welding [19,20], and improvement of mechanical properties [17,21,22], has been reported. Creating patterns on the surface of metallic glasses with laser irradiation has also been investigated in a few studies [23,24]. Huang et al. [23] increased the effective surface area of Zr-based metallic glasses through nanosecond pulsed laser irradiation under vacuum. The laser created hierarchical micro/nanostructures on $Zr_{41.2}Ti_{13.8}Cu_{12.5}Ni_{10}Be_{22.5}$ metallic glass, revealing that nanosecond laser irradiation is an effective method to generate such morphology, which is beneficial to expand the applications of metallic glasses as biomaterials and catalysts. Very recently, surface patterning to improve surface hydrophobicity was achieved with this method by the same group [24]. They changed the pulse overlap rate and successfully enhanced the contact angles between the substrate and water droplet from 96° for the as-cast sample to 144° for the laser-irradiated sample patterned at an overlap rate of 47%. Similar improvement of the surface wettability of metallic glass with laser irradiation was also reported by another group [17].

Although modifying hydrophobic properties by laser patterning has been achieved, the fabrication of optical gratings through laser irradiation for the metallic glass has yet to be reported. If such a process is established, optical gratings will be able to be fabricated simply, quickly, and cheaply on the surface of metallic glasses, which should promote the use of metallic glasses in optical devices/components. In this study, we demonstrate the patterning of $Zr_{55}Cu_{30}Al_{10}Ni_5$ metallic glass substrates using laser irradiation and investigate the

fabricated microstructure as well as the surface morphologies of laser-irradiated and non-irradiated areas. Grids with an interval of several tens of micrometers are prepared on the surface of the metallic glass substrates to assess the possibility of fabricating optical gratings on metallic glasses through laser irradiation.

2. Experimental Method

An alloy ingot with a nominal composition of $Zr_{55}Cu_{30}Al_{10}Ni_5$ (at.%) was prepared by arc melting a mixture of the pure metals in an argon atmosphere. The alloy was re-melted several times to ensure its homogeneity. Ribbon samples with a cross section of 0.05 × 4.3 mm were prepared by a melt-spinning technique. Disc samples with a diameter of 5 mm and thickness of around 1 mm were also prepared by cutting a cast rod into slices. The amorphous character of the samples was confirmed using X-ray diffraction (XRD; Bruker AXS D8 Advance) and transmission electron microscopy (TEM; Hitachi HF-2000) before use. The thermal properties of the samples were measured by differential scanning calorimetry (DSC; Perkin Elmer Diamond DSC) using a heating rate of 20 K/min. The surface of the disk samples was polished to a mirror-like finish before laser irradiation.

Laser irradiation was conducted in air (~20.6% O_2) with a Yb fiber laser (Sumitomo Electric SumiLas) with a wavelength of 1060 nm emitted from an oscillator. The laser oscillator was fixed above the sample stage (PI micos). The stage could be moved precisely in the X, Y, and Z directions (minimum movement step was about 5.5 nm) to draw any kind of pattern on the surface of the metallic glass sample. The laser scan rate, which was corresponded to the movement speed of the stage, and the electric current of the laser were

0.66 mm/s and 0.6 A, respectively. After laser irradiation, an optical microscope (OM; Olympus BX-51) and scanning electron microscope (SEM; JEOL JSM-6010LV) were used to investigate the appearance of the laser-patterned area. The microstructures on the front (laser-irradiated side) and back of the ribbon sample were characterized by XRD. Compositional analysis of a cross section of the disk sample after laser irradiation was conducted through energy-dispersive X-ray spectroscopy (EDS; JEOL JSM-6010LV). To confirm the precise patterning of the samples, a reflective diffraction test was performed using a custom-made diffraction apparatus (see Fig. 6). A green laser pointer with a wavelength of 532 nm was used to measure the interval between diffraction spots. The precise surface morphologies of the laser-irradiated and non-irradiated areas were visualized using a non-contact three-dimensional optical profiler (Taylor Hobson Talysurf CCI 6000).

3. Results and Discussion

The microstructure of the as-cast $Zr_{55}Cu_{30}Al_{10}Ni_5$ samples was examined with XRD and TEM (data not shown here). No detectable peaks or contrasts corresponding to crystalline phases were observed in both analyses, indicating that the obtained samples were completely amorphous. The DSC measurement of an as-cast ribbon sample showed that it possessed a glass transition temperature, crystallization temperature, and supercooled liquid region of 697, 769, and 72 K, respectively. Similar thermal properties were measured for the disk sample (data not included here).

Figure 1(a) shows an OM image of a $Zr_{55}Cu_{30}Al_{10}Ni_5$ sample after laser irradiation. Lines with a width of ~10 μm and interval of ~110 μm were successfully prepared on the surface of the metallic glass substrate. Figure 1(b) presents an SEM image of the lines formed on a disk sample. A line interval of ~220 μm was also fabricated by changing the stage movement.

Figure 2 exhibits XRD patterns of the front, where the laser was irradiated, and back of a ribbon sample patterned with a line interval of ~220 μm. For the laser-irradiated side, a broad peak associated with the amorphous nature of the substrate along with some small peaks corresponding to oxides/crystalline phases were observed. Most of the crystalline phases that formed during laser irradiation were zirconium oxides, including monoclinic zirconia (m-ZrO_2) and tetragonal zirconia (t-ZrO_2), while a very small amount of the crystalline phase $Cu_{10}Zr_7$ was also detected. Conversely, only a featureless pattern was observed for the back side. These XRD results indicate that laser irradiation induced formation of some oxides/crystalline phases in the amorphous substrate. Because the ribbon sample was only around 50 μm thick, one concern was that the heat from the laser irradiation would cause the

whole microstructure to crystallize and/or oxidize. Another concern was that heat accumulation during the several laser scans would cause the sample to fully crystallize. Indeed, Zhang et al. [25] reported that crystallization occurred preferentially in the heat-affected zone with an increasing number of laser scans. Our results showed that small amounts of crystalline phases/oxides formed only on one side of the ribbon sample, indicating that they presented locally and no marked crystalline growth occurred. The line interval of ~220 μm seemed to be large enough to dissipate sufficient heat from the sample to prevent further crystallization.

Figure 3 shows an SEM image of the cross section of a laser-irradiated disk sample. A clear hump was observed at the laser irradiated line (Point 2). Considering the XRD results, this may suggest that the oxygen in the ambient air reacted with certain elements, especially Zr, on the top surface of the substrate during laser irradiation. To investigate the compositions of the laser-irradiated line and substrate, EDS point analysis was performed; the results are presented in Table 1. The composition of the substrate (Point 1) was almost the nominal composition, although a small amount of oxygen (3.6%) was detected. In contrast, the laser-irradiated area possessed a different composition from the initial one. The laser-irradiated area had an oxygen content of 20.1%, which was much higher than that of the substrate. Also, a large increase of Al (i.e., 292%) was observed in the laser-irradiated region, whereas the Zr, Cu, and Ni contents were lower than the nominal compositions by 80%, 77%, and 58%, respectively. According to the Ellingham diagram, Al is much easier to oxidize than Zr, Cu, and Ni. This suggests that during laser irradiation in air, material flow of Al occurred preferentially and a stable Al_2O_3 layer formed on the surface of the laser-irradiated area.

However, the peak signal of Al_2O_3 was not clearly observed in the XRD pattern of the laser-irradiated sample. This is because a small amount of oxide may exist only on the top surface of the sample; therefore, it was difficult to detect by XRD. Similar results, namely, an Al_2O_3 layer forming on the top surface of metallic glasses during oxidation experiments, were also reported by Tam and colleagues for $Cu_{58.1}Zr_{35.9}Al_6$ ternary systems [26]. Such an Al_2O_3 thin layer was also confirmed in our previous study through auger electron spectroscopy [27].

To prepare finer patterns for use as optical gratings, a grid with an interval of several tens of micrometers was fabricated on the surface of a disk sample, as illustrated in Fig. 4. Both parallel and perpendicular lines were well fabricated by precisely controlling the stage movement. The upper inset is an EDS map that reveals the presence of oxygen over the whole area. A clear grid is also seen in the map, indicating that the oxides were locally present along the laser-irradiated lines. The bottom inset shows an enlarged image of the grid, which confirmed that the gird interval was around 27 μm.

Figure 5 presents the XRD results for the line-patterned surface of the disk sample with a grid interval of around 27 μm. Peaks corresponding to m-ZrO_2, t-ZrO_2, $Cu_{10}Zr_7$, and also $NiZr_2$ were superimposed on the broad peak from the amorphous substrate. The intensity of the $Cu_{10}Zr_7$ peak was higher than that of the ribbon sample with a grid interval of around 220 μm (see Fig. 2). This suggests that the higher density of laser irradiation prevented sufficient heat release, resulting in crystalline growth. Also, the $NiZr_2$ phase was detected on the surface of the finer grid, which was not detected for the ribbon sample. The $Cu_{10}Zr_7$ and $NiZr_2$ crystalline phases were also observed in the same alloy system reported by Zhang et al. [25]. In their paper, these phases formed during the laser scanning of five-layer deposits of

$Zr_{55}Cu_{30}Al_{10}Ni_5$ powder in vacuum. Although the ambient conditions in their experiment were different from those in ours, in which the laser irradiation was performed in air, the same crystalline phases were observed. This indicates that heat accumulation caused the formation/growth of these crystalline phases. The finer grid had a line interval of only ~27 μm, which is smaller than the thickness of the ribbon sample (50 μm), so a heat-affected zone may form near the scanning lines. Subsequent laser scanning could then facilitate the nucleation/growth of crystals. It should be noted that the amorphous phase was still present on the surface of the metallic glass substrate patterned with a fine grid.

To investigate the periodicity and accuracy of the pattern, a reflective diffraction test was conducted with custom-made diffraction apparatus to observe the diffraction spots from the surface of the sample. The relationship between the grating period d, diffraction angle θ, and wavelength λ can be described by Bragg's law (see Fig. 6(a)),

$$d\sin\theta = n\lambda\,, \quad \cdots \quad (1)$$

where n is the diffraction order. Here, $\sin\theta$ was geometrically calculated using the following equation (see Fig. 6(a)),

$$\sin\theta = \frac{X}{\sqrt{L^2+X^2}}, \quad \cdots \quad (2)$$

where X is the distance between the center of one diffraction spot and that of another and L is the length from the surface of the sample to the measurement point. Combining equation (1) and (2) gives equation (3),

$$d = \frac{\sqrt{L^2+X^2}}{X} \cdot n\lambda. \quad \cdots \quad (3)$$

Figure 6(b) shows a photograph of the custom-made diffraction apparatus and the obtained spots. Many diffraction spots appeared on the ruler in two dimensions. In the present study,

for simplicity, n=1 was considered (X and θ are denoted as X_1 and θ_1, respectively). The measured X_1 was 0.25±0.02 cm. Each obtained parameter is listed in Table 2. Equation (3) gave a calculated d of 26.4±2.3 μm, which was almost the same as that measured from the SEM image (~27 μm). This result clearly suggests that the diffraction spots originated from the laser-patterned lines, indicating that we successfully fabricated a line pattern with excellent periodicity and accuracy on the surface of a metallic glass substrate.

Figure 7(a) presents the precise surface morphology mapping of laser-irradiated and non-irradiated areas obtained with a three-dimensional optical profiler. The area not irradiated by the laser was almost flat after the irradiation of the sample. In contrast, ridges, as already observed in the cross-sectional SEM image in Fig. 3, were seen in the laser-irradiated areas. Hollows were observed next to the ridges, suggesting that material flow occurred in the laser-irradiated region. The laser-irradiated area may liquidize during irradiation and then subsequently solidify. The highest area was detected at the center of the laser-irradiated line (orange), while the lowest was at the edge (black), which means that the materials moved from the edge of the irradiated line to the center. Figure 7(b) reveals the surface morphology of a cross section of the sample. The x- and y-axes indicate the distance from a certain point and the height from the substrate, respectively. From this figure, an average height/depth of around 0.5 μm from the substrate was measured. Huang et al. [23,24] observed similar morphology after laser irradiation of the surface of metallic glass, and also discussed the mechanism of why such a morphology was created, although the height was quite different (around 2 μm). In their case, the laser was overlapped by 29%–82% during each scan. The preceding scan created a ridge with increasing material flow resistance, which may increase

the height of the ridge during the succeeding scan. In contrast, in our experiment, because each laser scan was isolated, the resistance to material flow was not increased much, so the height of the ridge/hollow was smaller. Furthermore, the interval between peaks was around 25 to 30 μm, consistent with that observed in the SEM image (see Fig. 4) and calculated from the diffraction spots (see Table 2). This result suggests that the periodic ridges with a height of 0.5 μm created the diffraction spots in Fig. 6 by acting as a reflective grating.

To demonstrate the possibility of using the patterned surface as an optical grating, its optical properties were investigated. Figure 8(a) shows a photograph of the sample taken at a certain angle under a fluorescent light. A color gradation that was ascribed to the interference of visible light was clearly present in the patterned region with an area of a few millimeters squared. The general formula of diffraction in the case of incident light entering from the oblique direction is expressed as (see Fig. 8(b)) [28],

$$d(\cos\varphi_1 - \cos\varphi_2) = n\lambda, \ \cdots \ (4)$$

where φ_1 and φ_2 are the incident and diffraction angle, respectively. This equation is simply equation (1) when φ_2 and φ_1 in equation (4) are 90° and 90°−θ, respectively. Thus, φ_2 can be obtained from equation (5) [27],

$$\varphi_2 = \cos^{-1}\left(\cos\varphi_1 - \frac{n\lambda}{d}\right). \ \cdots \ (5)$$

It is clear that φ_2 changes with λ. Namely, different colors (e.g., purple, green, red) will diffract different angles (e.g., φ_I, φ_{II}, φ_{III} in Fig. 8(c)). As the wavelength increases, the diffraction angle also increases, resulting in the gradation from purple at the back to the red at the front of the patterned sample. The appearance of this structural color gradation proves that optical gratings were fabricated on the surface of the sample through laser irradiation.

As mentioned before, although many optical gratings have been fabricated by superplastic forming [10,11], generating structural color on the surface of metallic glass through laser irradiation had never been reported. Our *d* is several tens of micrometers; patterning down to the nanometer scale is challenging but desirable because the decrease of *d* increases the grid number in a certain area, raising the reflection intensity from the incident light and resulting in an optical grating with higher efficiency/performance. However, our present study showed that it is possible to fabricate a grating on the surface of metallic glass using laser irradiation. Our findings provide useful information for practical applications of optical devices/components and sensor technologies.

4. Conclusions

Surface patterning of $Zr_{55}Cu_{30}Al_{10}Ni_5$ metallic glass ribbon and disk samples with laser irradiation was demonstrated with the aim of fabricating optical gratings. Our findings were as follows:

1. Periodic lines with intervals of ~27 to ~220 μm were successfully produced on the surface of metallic glass samples.
2. XRD results showed that oxides (m-ZrO_2, t-ZrO_2) and crystalline phases ($Cu_{10}Zr_7$, $NiZr_2$) were present together with the amorphous phase on the surface of the laser-irradiated samples.
3. The EDS analysis of a cross section of a disk sample revealed that high amounts of aluminum (292% of the nominal aluminum composition) and oxygen existed on the top surface of laser-irradiated area, suggesting that Al_2O_3 was generated there.

4. Grating periods calculated from the diffraction spots agreed well with the line interval measured by SEM, revealing that the spots originated from the patterned lines. The three-dimensional optical profiler data also showed that pairs of ridges and hollows with a height/depth of ~0.5 μm were present at the laser-irradiated lines. Such specific morphology created the diffraction spots by acting as a reflective grating.
5. Structural color gradation was successfully observed on the laser-patterned area under a fluorescent light, indicating that it is possible to fabricate optical gratings on the surface of metallic glasses with laser irradiation much easier, cheaper, and faster than with conventional superplastic forming.

Acknowledgments

We thank Natasha Lundin, PhD, from Edanz Group (www.edanzediting.com/ac) for editing a draft of this manuscript.

References

[1] M. F. Ashby, A. L. Greer, Scripta Materialia **54** (2006) 321-326.

[2] A. Inoue, B. L. Shen, C. T. Chang, Acta Materialia **52** (2004) 4093-4099.

[3] A. Inoue, B. Shen, A. Takeuchi, Materials Science and Engineering A **441** (2006) 18-25.

[4] L. Liu, C. L. Qin, Q. Chen, S. M. Zhang, Journal of Alloys and Compounds **425** (2006) 268-273.

[5] Y. Saotome, K. Imai, S. Shioda, S. Shimizu, T. Zhang, A. Inoue, Intermetallics **10** (2002) 1241-1247.

[6] J. Schroers, Advanced Materials **22** (2010) 1566-1597.

[7] G. Kumar, A. Desai, J. Schroers, Advanced Materials **23** (2011) 461-476.

[8] N. Li, E. Xu, Z. Liu, X. Wang, L. Liu, Scientific Reports **6** (2016) 39388.

[9] Y. Fukuda, Y. Saotome, N. Nishiyama, K. Takenaka, N. Saidoh, E. Makabe, A. Inoue, Journal of Vacuum Science and Technology B **30** (2012) 061602.

[10] J. P. Chu, H. Wijaya, C. W. Wu, T. R. Tsai, C. S. Wei, T. G. Nieh, J. Wadsworth, Applied Physics Letters **90** (2007) 034101.

[11] Y. Saotome, Y. Fukuda, I. Yamaguchi, A. Inoue, Journal of Alloys and Compounds **434-435** (2007) 97-101.

[12] M. Telford, Materialstoday **7** (2004) 36-43.

[13] M. Ishida, H. Takeda, D. Watanabe, K. Amiya, N. Nishiyama, K. Kita, Y. Saotome, A. Inoue, Materials Transactions **54** (2004) 1239-1244.

[14] S. Y. Chou, P. R. Krauss, P. J. Renstrom, Applied Physics Letters **67** (1995) 3114-3116.

[15] M. Hasan, G. Kumar, Scripta Materialia **123** (2016) 140-143.

[16] E. Williams, N. Lavery, Journal of Materials Processing Technology **247** (2017) 73-91.

[17] J. Fornell, E. Pellicer, E. G. Lecina, D. Nieto, S. Surinach, M. D. Baro, J. Sort, Applied Surface Science **290** (2014) 188-193.

[18] H. K. Lin, C. J. Lee, T. T. Hu, C. H. Li, J. C. Huang, Optics and Lasers in Engineering **50** (2012) 883-886.

[19] B. Shen, T. L. Shi, M. Li, F. Yang, F. Yan, G. L. Liao, Intermetallics **46** (2014) 111-117.

[20] L. Shao, A. Datye, J. Huang, J. Ketkaew, S. W. Sohn, S. Zhao, S. Wu, Y. Zhang, U. D. Schwarz, J. Schroers, Scientific Reports **7** (2017) 7989.

[21] B. Chen, S. Pang, P. Han, Y. Li, A. R. Yavari, G. Vaughan, T. Zhang, Journal of Alloys and Compounds **504S** (2010) S45-S47.

[22] Y. Wei, G. Xu, K. Zhang, Z. Yang, Y. Guo, C. Huang, B. Wei, Scientific Reports **7** (2017) 43948.

[23] H. Huang, N. Jun, M. Jiang, M. Ryoko, J. Yan, Materials and Design **109** (2016) 153-161.

[24] H. Huang, J. Yan, Journal of Micromechanics and Microengineering **27** (2017) 075007.

[25] Y. Zhang, X. Lin, L. Wang, L. Wei, F. Liu, W. Huang, Intermetallics **66** (2015) 22-23.

[26] C. Y. Tam, C. H. Shek, W. H. Wang, Reviews on Advanced Materials Science **18** (2008) 107-111.

[27] R. Yamada, N. Nomura, J. Junji, A. Kawasaki, Journal of Alloys and Compounds **727** (2017) 549-554.

[28] F. Wakabayashi, Bulletin of the National Science Museum, Tokyo. Series E **28** (2005) 21-30.

Captions

Figure 1: (a) Optical micrograph and (b) SEM image of the laser-irradiated lines formed on the surface of $Zr_{55}Cu_{30}Al_{10}Ni_5$ metallic glass samples.

Figure 2: XRD patterns obtained at the laser-irradiated front and back of a ribbon sample with a line interval of ~220 μm.

Figure 3: EDS point analyses of the cross section of a disk sample for the substrate (point 1) and laser-irradiated line (point 2).

Figure 4: SEM image of the fine grid fabricated on the surface of a sample. The upper inset is the EDS map of oxygen. An enlarged image is presented in the lower inset.

Figure 5: XRD pattern of the fine grid fabricated on the surface of a sample.

Figure 6: (a) Schematic illustration of the setup for the reflective diffraction test. Each parameter (λ, L, θ_1, X_1, d) is also shown. (b) Photograph of the custom-made diffraction apparatus. The enlarged image is a picture of the obtained spots.

Figure 7: (a) Three-dimensional surface image of the laser-irradiated and non-irradiated areas. (b) Cross-sectional morphology of the sample surface. In (a), the scale bar on the right side shows the height from the substrate.

Figure 8: (a) Photograph of a disk sample with a fine grid on its surface taken at a certain angle under fluorescent light. (b) Schematic illustration of a reflective grating where the incident light enters from the oblique direction. (c) The mechanism of the structural color gradation achieved from the fine grid.

Table 1: EDS point analyses of the cross section of a disk sample. Point 1 corresponds to the substrate and Point 2 to the laser-irradiated line.

Table 2: Parameters used to calculate the grating period *d* with equation (3).

Figure 1

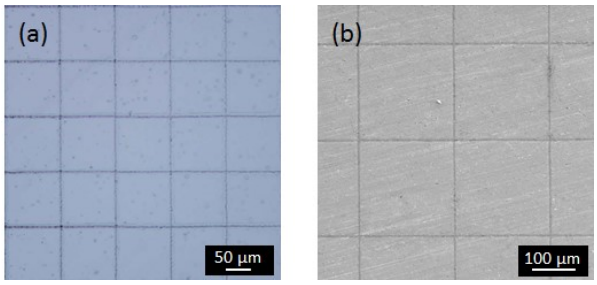

Figure 2

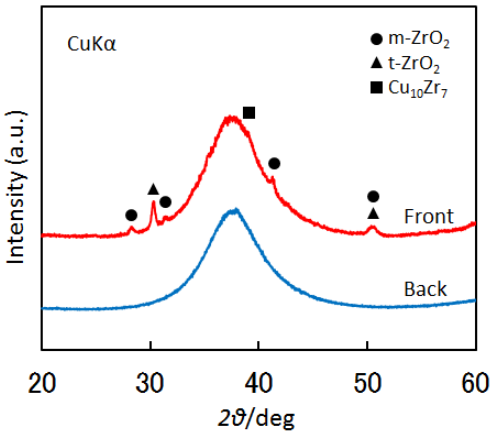
CuKα
● m-ZrO2
▲ t-ZrO2
■ Cu10Zr7
Intensity (a.u.)
Front
Back
20
30
40
50
60
2ϑ/deg

Figure 3

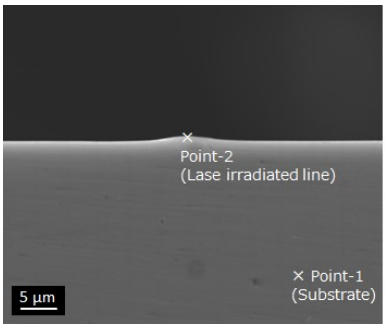

Figure 4

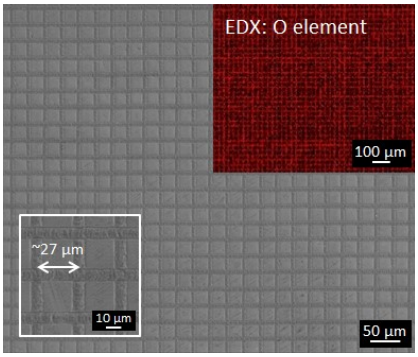

Figure 5

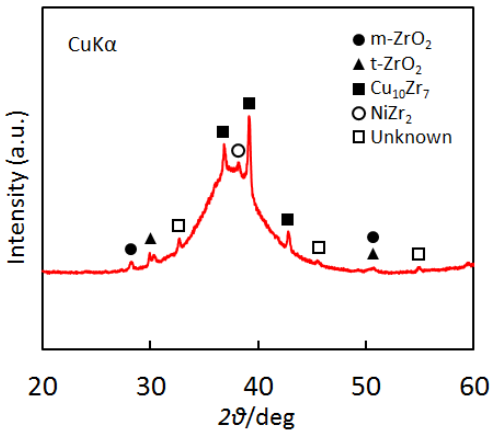
CuKα
● m-ZrO2
▲ t-ZrO2
■ Cu10Zr7
○ NiZr2
□ Unknown
Intensity (a.u.)
20
30
40
50
60
2ϑ/deg

Figure 6

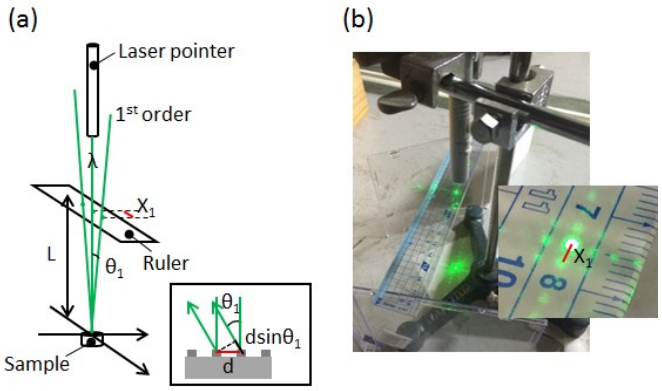
(a)
Laser pointer
1st order
λ
X1
L
θ1
Ruler
Sample
θ1
dsinθ1
d
(b)
X1

Figure 7

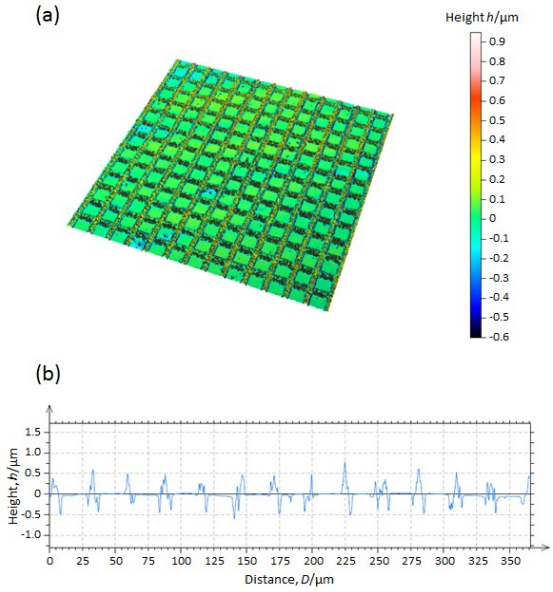
(a)
Height h/µm
0.9
0.8
0.7
0.6
0.5
0.4
0.3
0.2
0.1
0
-0.1
-0.2
-0.3
-0.4
-0.5
-0.6
(b)
Height, h/µm
1.5
1.0
0.5
0
-0.5
-1.0
0
25
50
75
100
125
150
175
200
225
250
275
300
325
350
Distance, D/µm

Figure 8

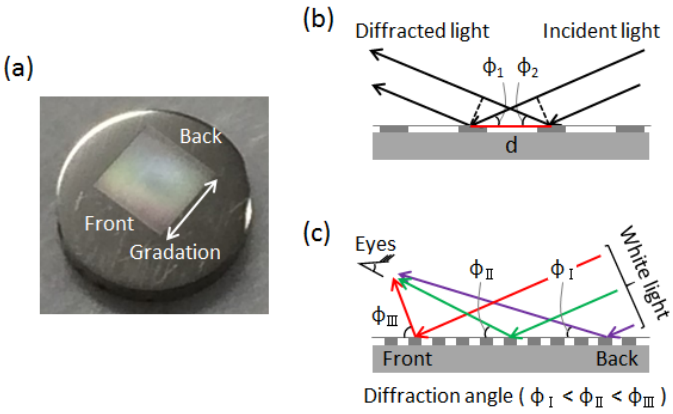
(a)
Back
Front
Gradation
(b)
Diffracted light
Incident light
ϕ_1 ϕ_2
d
(c)
Eyes
ϕ_{II}
ϕ_I
White light
ϕ_{III}
Front
Back
Diffraction angle ($\phi_I < \phi_{II} < \phi_{III}$)

Table1

Element	Nominal composition (at. %)	Point-1 (Substrate) (at. %)	Point-2 (Laser irradiated lines) (at. %)
Zr	55	53.4	35.2 (80 %)
Cu	30	30.4	18.5 (77 %)
Al	10	7.9	23.3 (292 %)
Ni	5	4.8	2.9 (58 %)
O	-	3.6	20.1

The numbers in parentheses denote the percentage of each element compared with the nominal composition.

Table 2

n (-)	λ (nm)	L (cm)	X_1 (cm)	d (μm)
1	532	12.4	0.25±0.02	26.4±2.3